Innate immune signalling of the zebrafish embryo

Stockhammer, O.W.

4 Transcriptome analysis of Traf6 function in the innate immune response of zebrafish embryos

Oliver W. Stockhammer[1], Han Rauwerda[2], Floyd R. Wittink[2], Timo M. Breit[2], Annemarie H. Meijer[1] and Herman P. Spaink[1]

1 Institute of Biology, Leiden University, Leiden, The Netherlands 2 MicroArray Department & Integrative Bioinformatics Unit, Swammerdam Institute for Life Sciences, University of Amsterdam, Amsterdam, The Netherlands

Abstract

TRAF6 is a key player at the cross-roads of development and immunity. The analysis of its *in vivo* molecular function is a great challenge since severe developmental defects and early lethality caused by *Traf6* deficiency in knock-out mice interfere with analyses of the immune response. In this study we have used a new strategy to analyse the function of Traf6 in a zebrafish-Salmonella infectious disease model. In our approach the effect of a Traf6 translation-blocking morpholino was titrated down to avoid developmental defects and the response to infection under these partial knock-down conditions was studied using the combination of microarray and next generation sequencing technology. Transcriptome profiling of the traf6 knock-down allowed the identification of a gene set whose responsiveness during infection is highly dependent on Traf6. Expression trend analysis based on the resulting data-sets identified nine clusters of genes with characteristic transcription response profiles, demonstrating Traf6 has a dynamic role as a positive and negative regulator. Among the Traf6-dependent genes was a large set of well known anti-microbial and inflammatory genes. Additionally, we identified several genes of which a role in the immune system was not previously known to be Traf6-dependent, such as the fertility hormone gene *gnrh2* and the DNA-damage regulated autophagy modulator 1 gene *dram1*. With the use of the zebrafish embryo model we have now dissected the *in vivo* function of Traf6 in the innate immune response without interference of adaptive immunity.

Introduction

Microbial infections usually elicit a rapid and strong response of the host innate immune system. Pattern recognition receptors (PRRs), such as Toll-like receptors (TLRs) and NOD-like receptors (NLRs), enable the host to recognize pathogens by detecting conserved molecular patterns such as lipopolysaccharide (LPS), flagellin or peptidoglycan (1). Activation of these receptors will initiate the induction of pro-inflammatory cytokines and as a result a complex network of underlying signalling pathways is activated leading to a tailored inflammatory response with the ultimate goal of eradicating the pathogen. An essential protein transducing the signals emanating from various PRRs and cytokine receptors, including the TNF superfamily, TGFβ, IL-1/Toll-like and NOD-like receptors, is the TNF receptor-associated factor 6 (TRAF6) (2-5).

Initial studies demonstrated the ability of TRAF6 to bind to CD40, RANK and IRAK-1 and showed that NF-κB signalling via TLR4 was abolished by a dominant-negative form of TRAF6 (6-12). Analysis of TRAF6 deficient mice revealed a critical role of TRAF6 in osteoclast development and function. Furthermore, these studies indicated an essential role of TRAF6 in IL-1 signalling, as the activation of NF-

κB and JNK in response to IL-1 were absent in embryonic fibroblasts derived from TRAF6-deficient mice. Moreover, bone marrow-derived macrophages from these mutants displayed a diminished response to LPS, and dendritic cell development and function was impaired (13-15).

The molecular mechanism underlying signal transduction by TRAF6 upon infection is that TRAF6 exerts its function as a K63-specific RING finger E3 ligase. Upon activation of the TLR or the IL-1 receptor pathway, the association of MyD88 with the cytosolic part of the receptor results in the phosphorylation of IRAK-1 by IRAK-4. Subsequently, activated IRAK1 will bind to TRAF6 that will form a complex with the ubiquitin-conjugating enzymes Ubc13 and Uev1a resulting in the attachment of non-degradative K63-linked ubiquitin chains to TRAF6 itself and to NEMO, the regulatory component of the IKK complex upstream of NF-κB. Ubiquitination of TRAF6 will recruit the TAB2/3-TAB1-TAK1 complex resulting in the activation of TAK1. Subsequent activation of the IKK complex and MAP kinase cascades by TAK1 lead to the induction of pro-inflammatory cytokines by the NF-κB and AP-1 transcription factor complexes, respectively (16-19). In addition to the role of TRAF6 in innate immunity, TRAF6 function was also placed in the context of adaptive immunity. Mice containing a T-cell specific deletion of TRAF6 showed the inability to maintain CD8 memory T-cells due to defective AMP-activated kinase activation and mitochondrial fatty acid oxidation after growth factor depletion (20).

Traf6 deficiency in mice causes severe developmental defects and early death at 17–19 days postnatal, making *in vivo* infection studies challenging. Therefore, we have used a zebrafish embryo model to perform *in vivo* infection experiments. In recent years the zebrafish (*Danio rerio*) embryo system has emerged as a model to study vertebrate innate immunity, offering several advantages that complement mammalian model systems. External development and the transparent character of the zebrafish embryo, in combination with fluorescently labeled immune cells and bacteria, allows for study of host microbe interaction and inflammation processes in the living organism (21-28). Analysis of the immune system of the zebrafish revealed a fully developed innate and adaptive immune system showing significant similarities to the human equivalent (29-33). An active innate immune system is detectable already at day one of zebrafish embryogenesis (21, 34, 35). By contrast, a functionally mature adaptive immune system is not active during the first three weeks of zebrafish development establishing a clear temporal separation of the innate and adaptive immune system in the zebrafish embryo. (36-38). Therefore, the zebrafish model provides a convenient system for the *in vivo* study of the vertebrate innate immune response to infection independently from the adaptive immune response. Furthermore, morpholino based knock-down experiments facilitate the functional analysis of genes in the zebrafish embryo that otherwise lead to lethal defects in gene knock-out studies in mice. Moreover, many infection systems for zebrafish have been developed lately, allowing the analysis of gene functions under infection conditions (32, 39, 40).

Here we report on the transcriptional analysis of the innate immune response in Traf6 knock-down and control embryos upon a bacterial infection using a previously described *Salmonella enterica* serovar *Typhimurium* (hereafter referred to as *S. typhimurium)* infection model (22, 33). By titrating down the concentration of a translation blocking morpholino we could avoid effects of Traf6 knock-down on embryo development and study the response to infection under these partial knock-down conditions. Multifactorial analysis of microarray data and confirmation by RNA deep sequencing allowed the identification of a gene set whose responsiveness to *S. typhimurium* infection is highly dependent on Traf6 function. Therefore, while our study indicates a role of Traf6 in developmental processes, it clearly illustrates its importance in the innate immune defence in the zebrafish embryo system.

Results

System for analysis of innate immune functions of Traf6

To accomplish *traf6* knock-down zebrafish embryos were injected at the one cell stage with an ATG morpholino to prevent *traf6* mRNA translation. Initial titration experiments of the *traf6* morpholino elicited a concentration-dependent effect on embryo development showing phenotypical defects, such as body axis truncation and brain malformation, when the administered morpholino concentration exceeded 1mM. To avoid the strong interference of developmental defects, all infection assays were performed using a concentration of 1mM *traf6* morpholino considered as an incomplete knock-down of *traf6*. To be able to discriminate between the specific effect of the *traf6* knock-down and possible aspecific morpholino effects in our assay a control group was treated with a 5bp mismatch *traf6* morpholino. At 27hpf both groups were either immune challenged by injection of 250 cfu of a *S. typhimurium* wild type strain or mock injected with PBS. The transcriptional response was subsequently analysed at 8 hours post infection (hpi) (Fig. 1A). Initial analysis of the datasets demonstrated a robust response to the infection in the control as well as in the *traf6* knock-down group. At the UniGene cluster level a total of 3720 genes ($p<0.05$ and a fold change < -1.2 and > 1.2) were regulated upon bacterial challenge in the control group. In contrast, a reduced response showing a total of 2840 differentially regulated genes ($p<0.05$ and a fold change < -1.2 and > 1.2) was noticeable in the *traf6* knock-down group (Fig. 1B, supplemental Table I). The *S. typhimurium*-induced expression signatures of both the control and the *traf6* knock-down groups were consistent with the published results of Stockhammer *et al.* and include all genes previously validated by Q-PCR in that study (33). As shown by projection of the microarray data on a GenMapp of the TLR-signalling pathway, the *S. typhimurium*-induced gene sets of both groups included several TLR pathway components and downstream targets (Fig. 2, supplemental Table II). Furthermore, GO-analysis on the zebrafish gene identifiers by master-target testing on the level of Biological

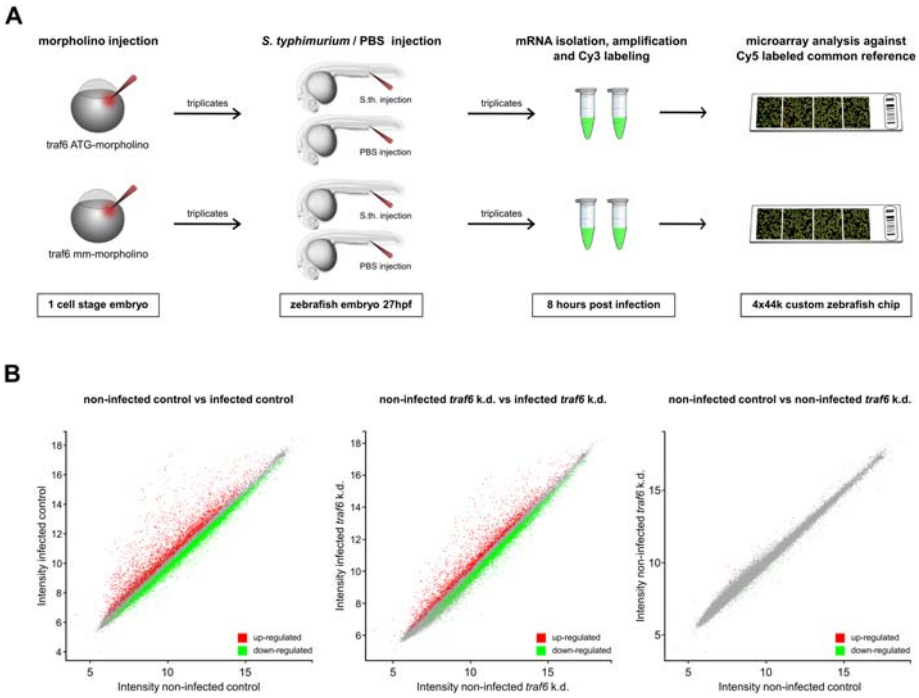

FIGURE 1. Schematic overview of the experimental setup (A) and scatter plot illustration of the transcriptional response of the various treatment groups (B). (A) Zebrafish embryos were either injected with a *traf6* ATG-morpholino or a 5bp mismatch (mm) morpholino at the first cell stage. At 27 hpf both groups were immune challenged by injection of 250 cfu of a *S. typhimurium* strain or mock injected with PBS. The transcriptional response was subsequently analysed at 8 hours post infection (hpi) using a common reference approach. The experiment was carried out in triplicate. (B) The scatter plots on the left side and in the middle show the transcriptional response upon *S. typhimurium* infection in the control (mm-morpholino) and *traf6* knock-down (k.d.) group respectively. The scatter plot on the right shows the response provoked by *traf6* knock-down independently of the infection.

Process revealed among others the GO-terms immune system process and response to stimulus as significantly ($p<0.05$) enriched in both groups (supplemental Table III). Interestingly, genes that were clustered under the GO-term reproduction were also significantly enriched in the up-regulated fraction. In contrast, only minor differences were provoked by *traf6* knock-down itself, indicating that our titration of the morpholino to avoid the developmental effect has been remarkably successful. In total 20 genes were up- and 35 genes were down-regulated by traf6 knock-down in the absence of infection ($p<0.05$, fold change $\leq$ -1.2 and $\geq$ 1.2) (Fig. 1B, supplemental Table IV). Among the group of up-regulated genes we identified genes such as *stc1 (stanniocalcin 1*, fc=2.62), a gene involved in $Ca2^{+}$ uptake in zebrafish, as well

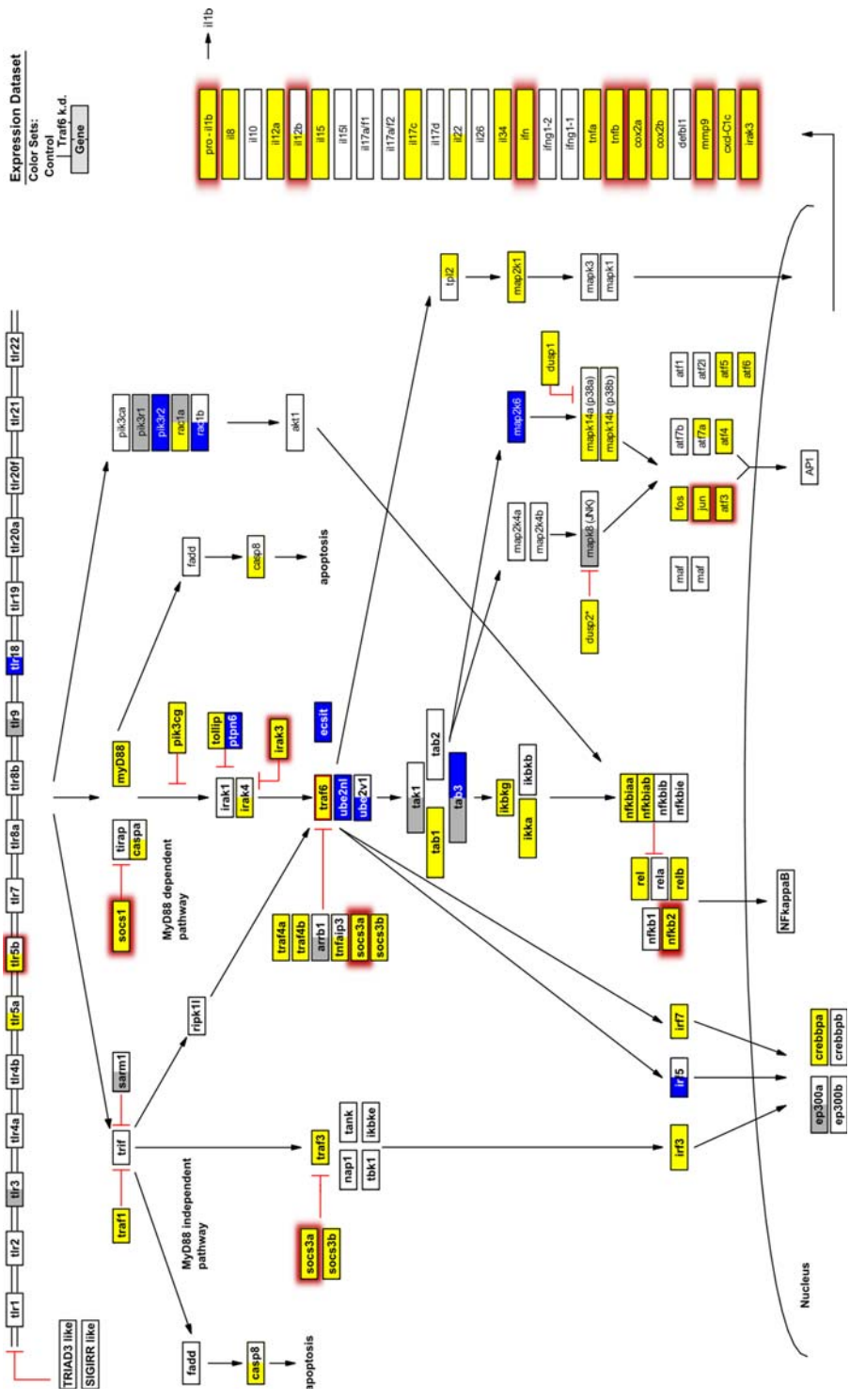
Expression Dataset
Color Sets:
Control
Traf6 k.d.
Gene
il1b
pro - il1b
il8
il10
il12a
il12b
il15
il15i
il17a/f1
il17a/f2
il17c
il17d
il22
il26
il34
ifn
ifng1-2
ifng1-1
tnfa
tnfb
cox2a
cox2b
defb1
mmp9
cxcl-C1c
irak3
tlr1
tlr2
tlr3
tlr4a
tlr4b
tlr5a
tlr5b
tlr7
tlr8a
tlr8b
tlr9
tlr18
tlr19
tlr20a
tlr20rl
tlr21
tlr22
TRIAD3 like
SIGIRR like
traf1
trif
sarm1
ripk1l
MyD88 independent pathway
fadd
casp8
apoptosis
socs3a
socs3b
traf3
nap1
tank
tbk1
ikbke
irf3
irf5
irf7
ep300a
ep300b
crebbpa
crebbpb
Nucleus
tirap
caspa
socs1
MyD88 dependent pathway
myD88
pik3ca
pik3r1
pik3r2
ras1a
ras1b
akt1
pik3cg
tollip
ptpn6
irak1
irak4
irak3
ecsit
traf6
ube2ni
ube2v1
tak1
tab1
tab2
tab3
ikbkg
ikka
ikkb
nfkbiaa
nfkbiab
nfkbib
nfkbie
rel
rela
relb
nfkb1
nfkb2
NFkappaB
fadd
casp8
apoptosis
traf4a
traf4b
arrb1
tnfaip3
socs3a
socs3b
tpl2
map2k1
mapk3
mapk1
dusp1
map2k6
mapk14a (p38a)
mapk14b (p38b)
map2k4a
map2k4b
mapk8 (JNK)
dusp2*
atf1
atf2
atf5
atf6
atf7b
atf7a
atf4
fos
jun
atf3
maf
maf
AP1

as *zgc:77734* (fc=2.57), showing similarities to the human DBI (diazepam binding inhibitor) gene. Examples of genes down-regulated by traf6 knock-down in the absence of infection are *or111-3* (fc=-3.8), a member of the fish odorant receptor family, and *he1a* (*hatching enzyme 1a*, fc=-2.68) as well as *rcv1* (*recoverin*, fc=-2.15) and *anterior gradient homolog 2* (*agr2*, fc=-1.89) (supplemental Table IV).

Statistical analysis of the effect of traf6 knock-down on the infection response

In order to find those genes that were specifically differentially regulated in the *traf6* knock-down group in comparison to the control group upon infection, the interaction term was analysed. Interaction is defined as the dependence of the effect of one factor (here gene knock-down by morpholino treatment) on the level of another factor (here immune challenge by infection). In terms of the analysis of variance (ANOVA) model, the interaction term measures the deviation from an expected value based on the additive combinations of the morpholino and infection means. A large positive deviation of this sort is called synergism, in which case the simultaneous morpholino and infection treatment gives rise to an expression level that deviates from the additive combination of the morpholino and infection treatment alone. A negative deviation, i.e. when the combined infection and morpholino application gives rise to a smaller effect than one could expect from the additive combination of the two effects separately, can be called interference. Synergy can be in the direction of overexpression or underexpression. In the former, a gene has a higher expression in the combined treatment than one could expect on the basis of the additive combination of the separate treatments. In the latter, a gene has an even lower expression in the combined treatment than one could expect on the basis of the additive combination of the separate treatments.

To specifically identify genes that were most highly dependent on Traf6 for their

FIGURE 2. GenMapp analysis of the immune response to *S. typhimurium* infection in the TLR pathway in control and traf6 knock-down embryos. Expression profiles of the control and *traf6* knock-down groups at the 8hpi time point (infected versus non infected, FDR corrected p-value <0.05 and fold changes ≥1.2 and ≤-1.2) were simultaneously mapped on the TLR pathway. Gene boxes are colour coded with the control morpholino treatment (Control) on the left and *traf6* knock-down (Traf6 k.d.) on the right side. Up-regulation is indicated in yellow, down-regulation in blue. The position of *traf6* in the pathway is highlighted by a red border of the gene box. Genes that failed the fold-change cut off are depicted in gray and genes that were not significantly regulated are represented in white. Highlighting of gene boxes by red shading indicates that the *S. typhimurium*-induced gene expression level was lower in *traf6* knock-down embryos than in control embryos, based on microarray expression trend analysis as well as RNAseq analysis. The pathway is based on knowledge of TLR signalling in mammalian species and it should be noted that most interactions remain to be experimentally confirmed in zebrafish.

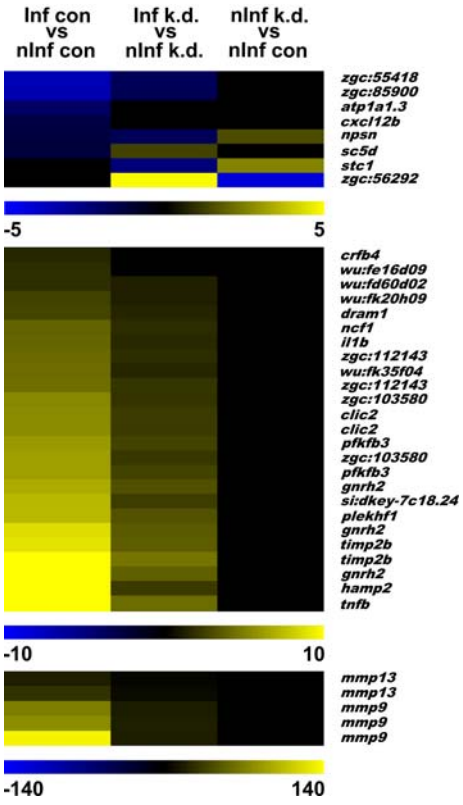

FIGURE 3. Heatmap showing the expression profiles of genes dependent on Traf6 during *S. typhimurium* infection as identified by interaction term analysis. Up-regulated expression is indicated in yellow, down-regulated expression in blue, and non-significantly changed expression in black. The level of up- or down-regulated expression is depicted by increasing brightness of yellow and blue colour, on three different scales for genes in different expression ranges. Note that several genes are represented by multiple probes on the microarray that showed significantly changed expression in the interaction term analysis. Gene descriptions and database identifiers are shown in Table 1. Column labels: infected control morpholino treated group (Inf con), noninfected control morpholino treated group (nInf con), infected *traf6* knock-down group (Inf k.d.), noninfected *traf6* knock-down group (nInf k.d.).

transcriptional response to a bacterial infection we examined all genes that were significant in the interaction term analysis with a stringent FDR-corrected p value smaller than 0.15 (Table I). The expression profiles of 28 identified genes corresponding to this criterion are shown in a heatmap (Fig.3). For the majority of these genes (20 out of 28) the *S. typhimurium*-induced gene expression levels were much lower in the *traf6* knock-down group than in the control group (Fig.3), indicating that the infection-mediated induction of these genes is dependent on *traf6*. Among these were several with a well established immune function like *hamp2*, *mmp9*, *mmp13*, *tnfb*, *il1b*, *ncf1*, *crfb4* and *zgc:103580*, the zebrafish ortholog of the human acute phase response gene serum Amyloid protein A. In addition to two members of the matrix metalloproteinase family (*mmp9* and *mmp13*), the group of 20 genes with a reduced infection response in *traf6* knock-down embryos also included the metalloproteinase inhibitor gene *timp2b* (*tissue inhibitor of metalloproteinase 2b*). This group also included *zgc:112143*, a gene homologous to the human *STEAP4* gene (also known as *TNFAIP9*, tumor necrosis factor alpha-induced protein 9), that we previously found to be induced with alternative splice forms during *Mycobacterium marinum* infection in adult zebrafish (41). On the other hand, the gene group showing a reduced infection response in *traf6* knock-down embryos also included genes that were pre-

Table I. Genes dependent on Traf6 during Salmonella infection*

Gene Symbol	Description	P-value	UniGene ID	ENS50 ID	K-means cluster	RNAseq
gnrh2	gonadotropin-releasing hormone 2	0.06	Dr.84757	ENSDARG00000044754	8	+
clic2	chloride intracellular channel 2	0.06	Dr.84618	ENSDARG00000010625	8	+
hamp2	hepcidin antimicrobial peptide 2	0.08	Dr.89447	ENSDARG00000053227	8	+
zgc:56292	similar to thyroid hormone receptor interactor 10	0.09	Dr.79814	ENSDARG00000028524	1	n.d.
pfkfb3	6-phosphofructo-2-kinase/fructose-2,6-biphosphatase 3	0.09	Dr.78868	ENSDARG00000001953	8	+
timp2b	tissue inhibitor of metalloproteinase 2b	0.09	Dr.81512	ENSDARG00000075261	8	+
dram1	DNA-damage regulated autophagy modulator 1	0.09	Dr.77501	ENSDARG00000045561	7	+
zgc:112143	STEAP family member 4 homolog	0.09	Dr.76505	ENSDARG00000055901	7	+
crfb4	cytokine receptor family member b4	0.11	Dr.14717	ENSDARG00000068711	7	+
wu:fk20h09	similar to pyruvate dehydrogenase complex, component X	0.11	Dr.140666		7	n.a.
zgc:103580	serum amyloid A1 homolog	0.11	Dr.13131	ENSDARG00000045999	7	+
cxcl12b	chemokine (C-X-C motif) ligand 12b	0.11	Dr.27045	ENSDARG00000055100	9	+
il1b	interleukin 1, beta	0.11	Dr.30443	ENSDARG00000005419	7	+
sc5d	sterol-C5-desaturase	0.11	Dr.119848	ENSDARG00000044642	4	-
mmp13	matrix metalloproteinase 13	0.12	Dr.81475	ENSDARG00000012395	7	+
mmp9	matrix metalloproteinase 9	0.12	Dr.76275	ENSDARG00000042816	8	+
tnfb	tumor necrosis factor b	0.12	Dr.94015	ENSDARG00000013598	8	+
wu:fk35f04	hypothetical protein containing S-100 domain	0.12	Dr.148687		7	n.a.
stc1	stanniocalcin 1	0.12	Dr.88421	ENSDARG00000058476	2	+
atp1a1a.3	ATPase, Na+/K+ transporting, alpha 1a.3 polypeptide	0.12	Dr.10713	ENSDARG00000039131	9	+
npsn	nephrosin	0.12	Dr.79156	ENSDARG00000010423	2	-
wu:fd60d02	transcribed locus	0.12	Dr.79931		8	n.a.
wu:fe16d09	transcribed locus	0.12	Dr.80006		7	n.a.
zgc:55418	similar to ABI gene family, member 3 (NESH) binding protein	0.12	Dr.14064	ENSDARG00000071095	9	+
zgc:85900	olfactomedin 2 like	0.14	Dr.85843	ENSDARG00000007015	9	+
ncf1	neutrophil cytosolic factor 1	0.14	Dr.2973	ENSDARG00000033735	8	+
plekhf1	pleckstrin homology domain containing, family F	0.14	Dr.80998	ENSDARG00000027852	8	+
si:dkey-7c18.24	hypotetical protein	0.14	Dr.104301	ENSDARG00000041433	7	+

* Listed genes were identified by interaction term analysis. Significance cut off values were set to p<0.15 (FDR). All genes indicated as + were confirmed by RNAseq analysis, whereas genes indicated as – were not. Four genes indicated as not applicable (n.a.) lacked an ENSDART identifier and could therefore not be verified by RNAseq analysis. For one gene indicated as not detectable (n.d.) not enough RNA sequence reads were obtained (< 1 mapped reads per million total reads). K-means cluster identifiers refer to Figure 5.

viously not linked to immune function or TRAF6 signalling like *plekhf1* (*pleckstrin homology domain containing, family F*), *clic2* (*chloride intracellular channel 2*), *pfkfb3* (*6-phosphofructo-2-kinase/fructose-2,6-biphosphatase 3*), *gnrh2* (*gonadotropin-releasing hormone 2*), and *dram1* (DNA-damage regulated autophagy modulator 1).

In addition to the 20 genes showing a reduced infection-mediated induction in *traf6* knock-down embryos, the statistical analysis also identified 4 genes (*cxcl12b*, *atp1a1a.3*, *zgc:55418* and *zgc:85900*) that appeared to be dependent on Traf6 for their negative regulation during infection. These genes were down-regulated by infection in control embryos but not or to a lower extent in *traf6* knock-down embryos (Fig.3, Table I). Four other genes showed a more complex dependency on Traf6, with opposite regulation in knock-down embryos and controls (*sc5d*) or with expression levels affected both in the absence and presence of infection (*zgc:56292*, *stc1*, *npsn*).

In conclusion, based on the interaction term analysis we identified genes that are dependent on Traf6 activity for their positive or negative regulation during *S. typhimurium* infection of zebrafish embryos.

Confirmation of Traf6-dependent genes by RNA deep sequencing

In order to confirm the microarray data we subjected the pooled RNA samples of

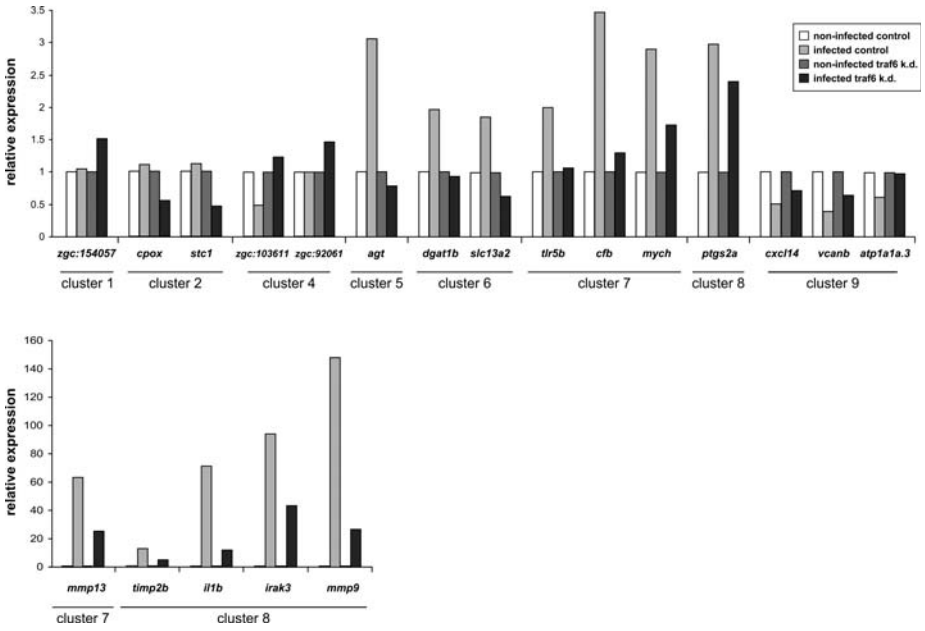

FIGURE 4. RNAseq validation of microarray results. RNAseq data are shown for representative examples of genes for which the microarray expression trend was confirmed by RNAseq read counts of the four treatment groups (non-infected control, infected control, non-infected *traf6* knock-down, infected *traf6* knock-down). Bars indicate the relative expression of the different treatment groups based on the number of mapped sequence reads per million of total reads. For every gene the value of the uninfected control group is set to 1 and the expression level of the gene in the treatment group is calculated relative to the control value. Two different scales are used for genes in different ranges of induction level upon *S. typhimurium* infection. Cluster numbers refer to the K-means clustering in Fig.5. The complete overview of genes for which the microarray expression trend was confirmed by RNAseq is given in supplemental Table VI

the three biological replicates of each treatment group to Illumina RNA sequencing (RNAseq). Approximately 15 million reads were obtained for each of the four RNAseq libraries (control, control infected, *traf6* knock-down, *traf6* knock-down infected) and approximately 10 million reads per library could be mapped to the Ensembl transcript database based on the Zv8 genome sequence. Next we compared the sequence read counts (mapped reads per million total reads) between the treatment groups (supplemental Table VI). For 21 of the 28 genes that were significant in the interaction term analysis, we found that the RNAseq data confirmed the microarray results. This included 16 of the 20 genes positively dependent on Traf6 during infection and all 4 of the genes negatively dependent on Traf6 during infection. Representative examples of these positively (*il1b*, *mmp9*, *mmp13*, *timp2b*) and negatively (*atp1a1a.3*, *cxcl12b*) regulated genes are shown in Fig. 4. In five cases the micro-

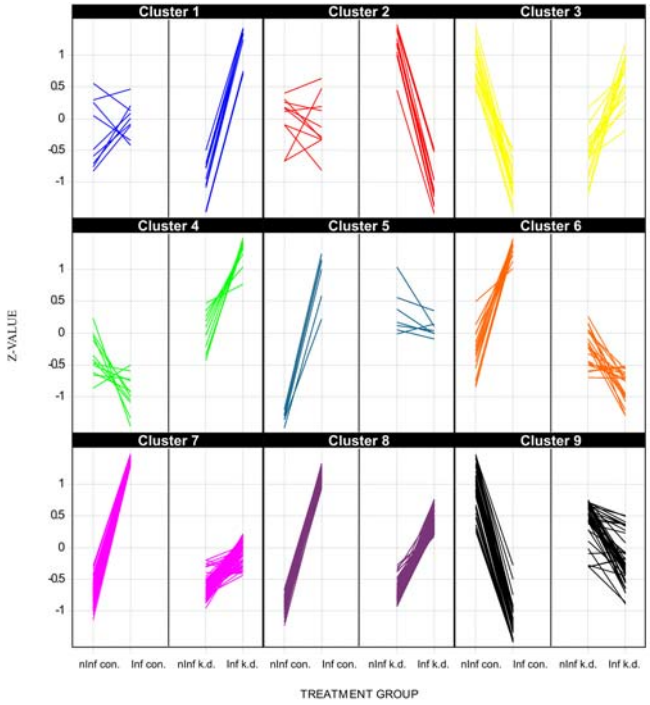

FIGURE 5. Trend analysis of the interaction term by K-means clustering. For a broader analysis of the effects of *traf6* knock-down all retrieved probes with an FDR-corrected p-value lower than 0.4 were clustered using the K-means cluster function in SPOTFIRE. All probes lacking a valid annotation were excluded from the analysis resulting in a final set of 376 probes. The identified trend in the control group is illustrated on the left side of each cluster expressed by the z-score of each probe between the noninfected (nInf con) and the infected (Inf con) control morpholino treated group. On the right side the corresponding trend of the noninfected (nInf k.d.) versus the infected (Inf k.d.) group under the *traf6* knock-down condition is illustrated. All probes that contribute to the distinct clusters are listed in supplemental table VI.

array data could not be validated by RNAseq because transcripts for these genes were not present in the Ensembl database or not enough RNAseq reads were obtained (< 1 mapped reads per million total reads). In only two cases, the RNAseq data did not confirm the microarray data. Both these cases (*sc5d*, *npsn*) were genes showing a complex dependency on Traf6 as described above. In conclusion, RNAseq analysis validated the interaction term analysis for most of the genes whose induction or repression during *S. typhimurium* infection was found to be dependent on Traf6.

Expression trend analysis

Since the knock-down conditions of Traf6 can be considered to be incomplete, we also wanted a broader overview of the effects of *traf6* knock-down in an expression

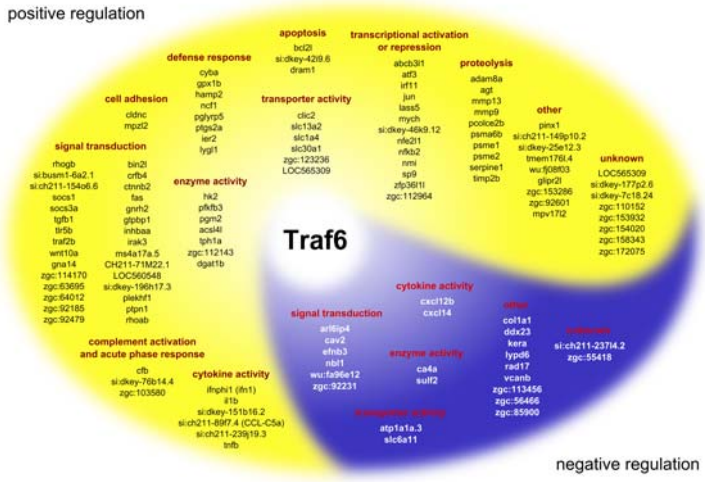

FIGURE 6. Schematic overview of the Traf6-dependent gene groups during *S. typhimurium* infection. Genes that are dependent on Traf6 for their induction during infection (positive regulation) are in the yellow area of the scheme and genes that depend on Traf6 for their repression (negative regulation) during infection are in the blue area. Genes positively regulated by Traf6 belong to clusters 5-8 in the microarray expression trend analysis in Figure 5, and genes negatively regulated by Traf6 belong to cluster 9. The microarray expression trend of all genes in the scheme was in agreement with RNAseq data.

trend analysis of the microarray data using a less stringent criterion: a FDR-corrected p-value of smaller than 0.4 retrieved from the interaction term. First, we analysed these probes by enrichment analysis based on Gene Ontology (GO) annotation. A significant enrichment was demonstrated for genes clustering under the biological process GO-terms immune system process ($p<0.05$), response to stimulus ($p<0.05$), and multi-organism process ($p<0.05$), demonstrating a clear effect of *traf6* knock-down on the immune response to *S. typhimurium* (supplemental Table V).

Following up the GO-term analysis, we subjected the selected probes to K-means cluster analysis, allowing for the visual discrimination between synergism and interference of the interaction term. Probes missing a valid annotation were excluded from the analysis. The remaining 376 probes, representing 233 genes, were categorized into 9 clusters (Fig. 5, supplemental table V). The microarray expression trends of 246 of these probes, representing 146 genes, were confirmed by the RNAseq data (supplemental table VI, with representative examples in Fig.4), indicating the validity of these results despite the use of a less stringent criterion in the interaction term analysis.

Genes indicated by clusters 1 and 2 were respectively up- or down-regulated upon infection under the *traf6* knock-down condition, whereas only minor and in the ma-

jority not significant changes were observed in the control group. These two clusters contain such genes as *zgc:1154057* (*transcriptional adaptor 2-like*) in cluster 1, and *cpox (coproporphyrinogen oxidase)* and *stc1* (*stanniocalcin 1*) in cluster 2 (supplemental Table VI, Fig. 4). Clusters 3 and 4 show an opposing trend in gene regulation upon infection between the control and *traf6* knock-down groups. Cluster 3 was not considered further, since regulation of genes in this cluster was generally not confirmed by the RNAseq data. Genes in cluster 4 were consistently up-regulated in the *traf6* knock-down group upon infection, while down-regulated or non-responsive in the control group, with examples such as *zgc:92061* (similar to keratin 17) and *tm7sf2* (transmembrane 7 superfamily member 2) (supplemental Table VI, Fig. 4). A common trend in gene regulation is observed in clusters 5 to 8, where infection leads to a consistent up-regulation in the control groups and weaker up-regulation (clusters 7 and 8) or unchanged expression (clusters 5 and 6) in the *traf6* knock-down groups. Finally, cluster 9 consists of those genes that were strongly down-regulated by infection in the controls, while showing a weaker or no down-regulation in *traf6* knock-down embryos.

For further analysis we concentrated on the genes that were dependent on Traf6 for their induction (clusters 5-8) or repression (cluster 9) during *S. typhimurium* infection. From the total of 124 genes with Traf6-dependent induction and 32 genes with Traf6-dependent repression, the microarray expression trend of 105 and 22 genes, respectively, could be confirmed by the RNAseq data (supplemental table VI, with representative examples in Fig.4). We categorized these Traf6-dependent genes into functional groups based on gene ontology terms and using references to gene function of their mammalian homologs in the NCBI Entrez Gene database (Fig.6). A notable fraction of the Traf6-dependent infection-induced genes play a well established role in the immune response, for example as cytokines or interferons (e.g. *il1b*, *tnfb*, *CCL-C5a*, *ifnphi1*), in complement activation or the acute phase response (e.g. *cfb*, *zgc:103580*), in prostaglandin biosynthesis (*pgts2a*), or in microbial killing (e.g. *ncf1*, *hamp2*). Many of the Traf6-dependent infection-induced genes are involved in signal transduction and transcriptional activation or repression. This includes the *tlr5b* gene, important for the response to flagellin, negative regulators of TLR-signaling (*irak3*, *socs3a*) as well as transcription factors (*atf3*, *jun*, *nfkb2*) activated by the TLR pathway (Fig.2, Fig.6). Other examples of Traf6-dependent signal transduction genes include *fas* (*TNF receptor superfamily, member 6*), *tgfb1* (*transforming growth factor, beta 1*), *ctnnb2* (beta-catenin2), *wnt10*a, and small gtpase genes (*rhogb*, *rhoab*). In addition to the above-mentioned Traf6-dependent members of the matrix metalloproteinase family (*mmp9* and *mmp13*) and metalloproteinase inhibitor gene (*timp2b*), the induction of several other genes involved in proteolysis was Traf6-dependent (e.g. *adam8a*, *agt*, *psme1/2*, *serpine1*). Finally, Traf6-dependent infection-induced gene groups were linked to apoptosis (e.g. *bcl2l*, *dram1*), cell adhesion (e.g. *cldnc*), transporter activity (e.g. *clic2*, *slc13a2*), or encoded enzymes involved in metabolic processes (e.g. *acsl4l*, *pfkfb3*, *dgat1b*) (Fig. 6).

Not only the infection-induced gene groups, but also the gene groups that were dependent on Traf6 for their repression during infection included genes for cytokines (*cxcl12b*, *cxcl14*), transporters (*atp1a1a.3*, *slc56a11*), enzymes (*ca4a*, *sulf2*) and signal transduction proteins (e.g. *efnb3*, *nbl1*). In addition, several other genes, for example *vcanb*, encoding a member of the hyaluronan (HA)-binding proteoglycans, were repressed by infection in a Traf6-dependent manner (Fig.6).

Taken together, based on the expression trend analysis of the microarray data and validation by RNAseq, we conclude that Traf6 has a dynamic role as a positive and negative regulator of genes responsive to *S. typhimurium* infection in zebrafish embryos, including a large set of well known anti-microbial and inflammatory genes as well as genes not previously linked to the immune response or to Traf6 function.

Discussion

The fact that TRAF6 is a key player at the cross-roads of development and immunity makes the analysis of its *in vivo* molecular function a great challenge (13, 14, 47). Severe developmental defects and early lethality caused by *Traf6* deficiency in knock-out mice interfere with analyses of the immune response. In this study we have developed a new approach to analyse the function of Traf6 in a zebrafish acute infectious disease model. In this approach the effect of a Traf6 translation-blocking morpholino was titrated in such a way that developmental defects were brought back to an identifiable non-dominant factor in the transcriptome analyses. The results show that, even under partial knock-down conditions, it was possible to identify a gene set (Table I) whose responsiveness during *S. typhimurium* infection is highly dependent on Traf6. In addition, expression trend analysis identified nine clusters of genes with characteristic transcription response profiles, demonstrating that Traf6 has a dynamic role as a positive and negative regulator. We have confirmed the data from microarray experiments with whole transcriptome shotgun sequencing (RNA-seq). This is one of the first times that this novel deep sequencing approach has been used for quantitative transcriptome profiling (48, 49). The results show that this complementary technique gives good support for the identified Traf6-dependent infection-responsive gene set, confirming Traf6-dependent induction of 105 genes and Traf6-dependent repression of 22 genes during *S. typhimurium* infection. In addition, especially since this is the first time that RNA-seq technology is used for infectious disease studies, these data represent a great wealth of disease-induced transcript information that will be of great value for future studies.

Among the genes that are highly dependent on Traf6 for their induction in response to *S. typhimurium* infection a subset of well known immune system-associated genes such as *il1b*, *mmp9, mmp13*, *hamp2,* and *tnfb* was found, demonstrating a specific *in vivo* effect of Traf6 on the innate immune response. Previously we could show that *il1b* and *mmp9* are downstream targets of the zebrafish TLR-pathway. The

dependency of the expression of these genes on Traf6 is consistent with this study and supports the specificity of the morpholino knock-down (33). It was shown in mouse that MMP-9 can also be activated upon RANKL stimulation via TRAF6, p38 and ERK1/2 (50). RANKL is a member of the tumor necrosis factor (ligand) superfamily and is an important activator of osteoclasts, cells involved in bone resorption. Although osteoclasts only develop in zebrafish larvae after several weeks it is not unlikely that these pathways are conserved during embryonic development (51). Several of the other Traf6-dependent genes that are linked to the TLR/IL1R-pathway are also corroborated in other model systems. It was shown that the regulation of hepcidin (HAMP1) is facilitated via the TLR-pathway in mice-derived macrophages upon bacterial infection (52). Another example shown in mouse is that activation of MMP-13 through the IL1-signalling pathway was strongly impaired after *traf6* knock-down (53). Interestingly, also the induction of a tissue inhibitor of metalloproteinase function, Timp2b was dependent of Traf6 during zebrafish embryo infection. The expression of *timp2b* was also found to be induced during mycobacterium infection in zebrafish embryos, which was suggested to function as a compensatory response to increased *mmp9* activity (54). Furthermore, human TIMP2 has been linked to cancer progression and has been found to be a marker for dendritic cell response to HIV infection (55). The known immune response genes that we showed to be induced in a Traf6-dependent manner also included components of the TLR-signalling pathway, such as *tlr5b* and *irak3*. It remains a question whether the regulation of the above mentioned genes is mediated via the TLR-pathway itself or via another Traf6-directed pathway. For instance Salmonella infection also regulated *tgfb1* in the TGF-beta pathway in a Traf6-dependent manner. Therefore, the poorly understood interrelatedness of the TGF-beta and TLR signaling pathways remains an important subject for future investigations.

Other Traf6-dependent infection induced genes, such as *dram1* (*DNA-damage regulated autophagy modulator 1*) and *gnrh2* (*gonadotropin releasing hormone 2)*, have until know not been directly associated with TRAF6 function. Human homologs of *dram1* are activated by p53 as a requirement to induce autophagy and damage-induced programmed cell death (56, 57). As recently highlighted in several studies, the autophagy pathway is also important for the control of intracellular pathogens and therefore the link with Traf6 function is relevant for Salmonella infection (58, 59). In the zebrafish embryo *gnrh2* has been linked to central nervous system development (60). However, next to the well established function of GnRH in mammalian reproduction, an immune regulatory function was suggested as well (61, 62). In fact, Tanriverdi et al. have discussed that immune and reproductive function are intrinsically linked in a so-called hypothalamic-pitutary-gonadal axis (60). Recently it was shown that GnRH treatment of mice macrophages *in vitro* leads to elevated Ca2+ uptake and an impaired generation of NO and suppression of iNOS after LPS/INF-γ treatment (63). A function of Traf6 in Ca2+ homeostasis is suggested by the fact that there is an interference effect of *traf6* knock-down and *S. typhimurium* in-

fection on *stanniocalcin* (*stc1*) regulation. The mammalian homolog of *stanniocalcin* is involved in inhibition of transendothelial migration of human macrophages and T-lymphocytes (64). In addition *stanniocalcin* was also shown to stimulate osteoblast differentiation in rat calvaria cells (65). In a broader sense, Traf6 is probably involved in other ion transport processes. For instance the induction of *chloride intracellular channel 2* (*clic2*) by Salmonella infection is highly dependent of Traf6 function. Furthermore, the negative regulation of *ATPase, Na+/K+ transporting, alpha 1a.3 polypeptide* (*atp1a1a.3*) during *S. typhimurium* infection is blocked by *traf6* knock-down.

In addition to the annotated genes we also have identified Traf6 targets of which no annotation could be derived either for zebrafish, mouse or human orthologs (Supplemental Tab. VI, Fig. 6). Even domain searches could not identify a possible function. Since the expression levels of some of these genes are both strongly affected by Salmonella induction at early time points (33) and are strongly dependent on Traf6 function, the further study of the function of these genes in the vertebrate immune system is of great interest.

Interestingly, we find the induction of several metabolic genes to be dependent on Traf6 function during Salmonella infection in one-day old embryos, suggesting a possible role in the immune response. For example, expression of *6-phosphofructo-2-kinase* (*pfkfb3*), *hexokinase 2* (*hk2*), and *diacylglycerol O-acyltransferase homolog 1b* (*dgat1b*) were induced during infection in a Traf6-dependent manner. Furthermore, the induction of an ortholog of STEAP4 (*zgc:112143*), which has been shown to play a role in integration of inflammatory and metabolic responses, is also dependent on Traf6 (66). We previously found this gene also to be induced by mycobacterium infection in zebrafish (41). The expression trend analysis shows that *pfkb3*, *hk2* and *zgc:111243* cluster together with several of the above mentioned inflammatory genes such as *mmp9*, *mmp13*, *il1b* and *tnfb* (Fig. 5). Other metabolic functions might also play a role during infection since our analyses only show the minimal contribution of Traf6 to immunity. This is because functions that play an equally important role in immunity and development cannot confidently be analyzed in our method since we have titrated down the effect of the morpholino treatment to have a low effect on development.

It does not come as a surprise that after knock-down of Traf6 there is still a strong immune response to Salmonella infection, not only because the knock-down was incomplete but also because it can be expected that there are innate immune responses to Salmonella infection that are independent of Traf6, for example the chemotactic response to the bacterial infection site via G-protein coupled receptors. Furthermore, also within the TLR-dependent pathway there are possible signaling routes that might not be dependent on Traf6. For instance, the pathway of TLR4 signaling can lead to TRAF3 activation and subsequent stimulation of the interferon pathway via the IRF3 protein. It would therefore also be interesting to use our method to analyze other key factors such as TRAF3 and partners immediately downstream of the TRAF

family proteins such as TBK1 and TAB1/2/3. Such studies could show whether any of these factors might be partially redundant during the innate immune response.

Materials and Methods

Bacterial strains and growth conditions

S. typhimurium wild type (wt) strain SL1027, containing the DsRed expression vector pGMDs3, was used for the infection of zebrafish embryos (22). Bacteria were freshly grown overnight on LB agar plates supplemented with 100µg/ml carbenicillin and resuspended in phosphate-buffered saline (PBS) prior to injection.

Zebrafish husbandry

Zebrafish were handled in compliance with the local animal welfare regulations and maintained according to standard protocols (http://ZFIN.org). Embryos were grown at 28,5 -30 °C in egg water (60µg/ml Instant Ocean sea salts). For the duration of bacterial injections embryos were kept under anaesthesia in egg water containing 0.02% buffered 3-aminobenzoic acid ethyl ester (tricaine, Sigma).

Morpholino knock-down experiments

For morpholino knockdown experiments, morpholino oligonucleotides (Gene Tools) were diluted to desired concentrations in 1x Danieu's buffer [58 mM NaCl, 0.7 mM KCl, 0.4 mM $MgSO_4$, 0.6 mM $Ca(NO_3)2$, 5.0 mM HEPES; pH 7.6] containing 1% Phenol red (Sigma). To block translation of *traf6* mRNA we injected 1 nl (1 mM) per embryo of a morpholino specifically targeting the 5' UTR region including the start codon of *traf6* (5' GCCATATTGGCTCGGTACGGCCTC). To control for aspecific morpholino effects we used a 5 bp mismatch morpholino (1mM, 5' GCaATATTcGCTaGGTACaGCgTC).

Experimental design of the infection study

All infection experiments were performed using mixed egg clutches of ABxTL strain zebrafish. Embryos injected with the *traf6* morpholino and the 5bp mismatch morpholino were staged at 27 hours post fertilization (hpf) by morphological criteria and approximately 250 cfu of DsRed expressing *S. typhimurium* wild type bacteria were injected into the caudal vein close to the urogenital opening as described in Stockhammer et al. (33). As a control an equal volume of PBS was likewise injected. Pools of 20-40 infected and control embryos were collected 8 hours post infection (hpi). For the microarray analysis, the whole procedure was performed in triplicate on separate days.

RNA extraction

Embryos for RNA isolation were snap frozen in liquid nitrogen and subsequently

stored at -80°C. Total RNA from each sample was extracted using TRIZOL followed by a cleanup procedure with Rneasy Mini kit (Qiagen, Valencia, CA, USA), and a DNase treatment with RNase-Free DNase Set (Qiagen Valencia, CA, USA)). The RNA concentration was measured on a nanodrop ND-100 (NanoDrop Technologies Inc., Wilmington, DE, USA) and RNA quality was checked on an Agilent 2100 BioAnalyzer (Agilent Technologies, Palo Alto, CA, USA). Total RNA samples with an RNA integrity number (RIN) > 7 were used for further analysis. These assays were performed according to the manufacturer's protocols.

Illumina RNA sequencing

The total RNA of the three biological samples of each treatment group, previously used for the microarray analysis, was pooled using equal amounts of RNA. To perform transcriptome sequencing, RNAseq libraries were made from 4 µg of each sample, using the Illumina mRNA-Seq Sample Preparation Kit according to the manufacturer's instructions (Illumina, Inc. San Diego). An amount of 4 pmol of each library was sequenced in one lane with a read length of 51 nt on an Illumina GAII instrument (Illumina, Inc. San Diego). The raw data were deposited in the GEO database under submission number GSE21024. Sequence reads were mapped to Ensembl transcripts (Zv8. 56) using the CLCbio Genomics Workbench version 3.6.5 (www.clcbio.com).

Microarray design and hybridization

A custom zebrafish genome 4 x 44 K microarray (Agilent) containing slight modifications in regard to a previous described design was used (accession no. GPL10042 in the GEO database) (33). In short, a total of 600 new features based on deep sequencing results were added to the existing chip design resulting in 45219 features, including 43801 well-characterized genes and 1418 controls (41). The probes of the custom manufactured Agilent array have been reannotated by mapping all probes to the Unigene 114 (unique) sequences and the Ensembl 50 and Vega 32 transcripts using the BLAST algorithm. Technical handling of the microarrays was performed at the MicroArray Department (MAD) of the University of Amsterdam (Amsterdam, The Netherlands). In short, cyanine 3 and cyanine 5 labeled cRNA samples were prepared as described in the Amino allyl message AMP II manual (Ambion) using 0.5 ug purified total RNA as template for the reaction. Test samples were labelled with Cy3 and the common reference was labeled with Cy5. The common reference was composed by combining 1 ug of cRNA from each sample and chemical coupling of this pool with Cy5. Hybridization of 825 ng of Cy3 labeled test sample and 825 ng of Cy5 labeled common reference was performed overnight according to Agilent protocols at 65° C. Images of the arrays were acquired using an Agilent DNA MicroArray Scanner (Agilent Technologies, Palo Alto, CA, USA).

Data extraction and statistical analysis

Spot intensities were quantified with Feature Extraction 9.5.1 (Agilent) as the foreground median signal intensity. Further processing of the data was performed using R (version 2.5.0), the Bioconductor MAANOVA package (version 1.6.0) (42) and Spotfire (version 7.3).

All slides were subjected to a set of quality control checks, i.e. visual inspection of the scans, examining the consistency among the replicated samples by principal components analysis, testing against criteria for signal to noise ratios, testing for consistent performance of the labeling dyes, and visual inspection of pre- and post-normalized data with box plots and RI plots.

The data set concerned a two-factorial Latin square design, with the factors 'Morpholino treatment' (2 levels: treated and not treated) and 'Infection' (2 levels: treated and not treated). The design was completely balanced with 3 replicates each, so the experiment involved 12 observations per gene.

After log2 transformation the data was normalized by a global LOWESS smoothing procedure. The data was analyzed using a two-stage mixed analysis of variance (ANOVA) model (43). First, array, dye, and array-by-dye effects were modeled globally. Next, the residuals from this first model were fed into a gene-by-gene model in which we took 'Group', 'Array', and 'Dye' as factors of which 'Array' was modeled as random factor. 'Group' is defined by each unique Morpholino and Infection treatment combination. These residuals can be considered normalized expression values and used in the graphs to depict gene expression profiles. All changes were calculated from the model coefficients. For hypothesis testing a permutation based Fs test, which allows relaxation of the assumption that the data are normally distributed, was used (2,000 permutations). The significance of the differences between factor level means was tested using contrasts. To account for multiple testing, all P values were adjusted to represent a false discovery rate using the method of Benjamini and Hochberg (44). The raw data were submitted to the GEO database under accession number GSE20310.

Gene Ontology, pathway and cluster analysis

K-means clustering was performed using Spotfire (version 7.3) Cluster initialization was set to data centroid based search and similarity measure was set to Euclidian distance. Analysis was performed on the probes retrieved by interaction term analysis with a p-value lower than or equal to 0.4. All identifiers lacking a valid annotation were excluded from the analysis leading to a dataset of 376 probes.

Gene ontology (GO) analysis was performed using the GeneTools eGOn v2.0 web-based gene ontology analysis software (www.genetools.microarray.ntnu.no) (45). Master-target analysis was performed at the level of Unigene clusters (UniGene build #105). To test for enrichment or under representation at the level of GO criteria for Biological Process (BP) we compared the UniGene identifiers retrieved from

our analysis (targets) to all identifiers present on the chip (master). Identifiers tested are listed in supplemental Table I and IV for those genes that were regulated after infection in the control and *traf6* knock-down group as well as due to *traf6* knock-down alone. All identifiers that were retrieved from the interaction term analysis are listed in supplemental Table VI.

Pathway analysis was performed using the GenMapp software package (www.genmap.org) (46). Analysis was done at the level of UniGene clusters (*D.rerio* UniGene build #114). Significance cut-off was set at 1.2 fold change at P <0.05. Zebrafish homologs of the genes contributing to the TLR pathway were identified by either searching the ZFIN (http://zfin.org) database or the Gene and HomoloGene database of NCBI (http://www.ncbi.nlm.nih.gov) (supplemental Table II).

The following link has been created to allow review of record GSE21024:
http://www.ncbi.nlm.nih.gov/geo/query/acc.cgi?token=jhwzvcicksqqabm&acc=GSE21024
The following link has been created to allow review of record GSE20310:
http://www.ncbi.nlm.nih.gov/geo/query/acc.cgi?token=rxcjnswseookuvk&acc=GSE20310

Acknowledgments

We are grateful to Christiaan Henkel and Hans Jansen (ZFscreens B.V., the Netherlands) for help with RNAseq analysis and thank our group members for helpful discussions. We are also grateful to Davy de Witt, Ulrike Nehrdich and Karen Bosma for fish maintenance. This work was financially supported by the European Commission 6th Framework Programs ZF-TOOLS (LSHG-CT-2006-037220)

Supplementary Data

Supplementary tables can be found online at: http://www.mediafire.com/?sharekey=686efof919604e919bf8d6369220dcab43aecfabc95fc71da7b01fe6e4055ae3

References

1. Mogensen, T. H. 2009. Pathogen recognition and inflammatory signaling in innate immune defenses. *Clin Microbiol Rev* 22:240-273, Table of Contents.
2. Abbott, D. W., Y. Yang, J. E. Hutti, S. Madhavarapu, M. A. Kelliher, and L. C. Cantley. 2007. Coordinated regulation of Toll-like receptor and NOD2 signaling by K63-linked polyubiquitin chains. *Mol Cell Biol* 27:6012-6025.
3. Kobayashi, T., M. C. Walsh, and Y. Choi. 2004. The role of TRAF6 in signal transduction and the immune response. *Microbes Infect* 6:1333-1338.
4. Sorrentino, A., N. Thakur, S. Grimsby, A. Marcusson, V. von Bulow, N. Schuster, S. Zhang, C. H. Heldin, and M. Landstrom. 2008. The type I TGF-beta receptor engages TRAF6 to activate TAK1 in a receptor kinase-independent manner. *Nat Cell Biol* 10:1199-1207.
5. Yamashita, M., K. Fatyol, C. Jin, X. Wang, Z. Liu, and Y. E. Zhang. 2008. TRAF6 mediates Smad-independent activation of JNK and p38 by TGF-beta. *Mol Cell* 31:918-924.
6. Cao, Z., J. Xiong, M. Takeuchi, T. Kurama, and D. V. Goeddel. 1996. TRAF6 is a signal transducer for interleukin-1. *Nature* 383:443-446.
7. Ishida, T., S. Mizushima, S. Azuma, N. Kobayashi, T. Tojo, K. Suzuki, S. Aizawa, T. Watanabe, G. Mosialos, E. Kieff, T. Yamamoto, and J. Inoue. 1996. Identification of TRAF6, a novel tumor necrosis factor receptor-associated factor protein that mediates signaling from an amino-terminal domain of the CD40 cytoplasmic region. *J Biol Chem* 271:28745-28748.
8. Galibert, L., M. E. Tometsko, D. M. Anderson, D. Cosman, and W. C. Dougall. 1998. The involvement of multiple tumor necrosis factor receptor (TNFR)-associated factors in the signaling mechanisms of receptor activator of NF-kappaB, a member of the TNFR superfamily. *J Biol Chem* 273:34120-34127.
9. Muzio, M., G. Natoli, S. Saccani, M. Levrero, and A. Mantovani. 1998. The human toll signaling pathway: divergence of nuclear factor kappaB and JNK/SAPK activation upstream of tumor necrosis factor receptor-associated factor 6 (TRAF6). *J Exp Med* 187:2097-2101.
10. Wong, B. R., R. Josien, S. Y. Lee, M. Vologodskaia, R. M. Steinman, and Y. Choi. 1998. The TRAF family of signal transducers mediates NF-kappaB activation by the TRANCE receptor. *J Biol Chem* 273:28355-28359.
11. Darnay, B. G., J. Ni, P. A. Moore, and B. B. Aggarwal. 1999. Activation of NF-kappaB by RANK requires tumor necrosis factor receptor-associated factor (TRAF) 6 and NF-kappaB-inducing kinase. Identification of a novel TRAF6 interaction motif. *J Biol Chem* 274:7724-7731.
12. Tsukamoto, N., N. Kobayashi, S. Azuma, T. Yamamoto, and J. Inoue. 1999. Two differently regulated nuclear factor kappaB activation pathways triggered by the cytoplasmic tail of CD40. *Proc Natl Acad Sci U S A* 96:1234-1239.
13. Lomaga, M. A., W. C. Yeh, I. Sarosi, G. S. Duncan, C. Furlonger, A. Ho, S. Morony, C. Capparelli, G. Van, S. Kaufman, A. van der Heiden, A. Itie, A. Wakeham, W. Khoo, T. Sasaki, Z. Cao, J. M. Penninger, C. J. Paige, D. L. Lacey, C. R. Dunstan, W. J. Boyle, D. V. Goeddel, and T. W. Mak. 1999. TRAF6 deficiency results in osteopetrosis and defective interleukin-1, CD40, and LPS signaling. *Genes Dev* 13:1015-1024.
14. Naito, A., S. Azuma, S. Tanaka, T. Miyazaki, S. Takaki, K. Takatsu, K. Nakao, K. Nakamura, M. Katsuki, T. Yamamoto, and J. Inoue. 1999. Severe osteopetrosis, defective interleukin-1 signalling and lymph node organogenesis in TRAF6-deficient mice. *Genes Cells* 4:353-362.
15. Kobayashi, T., P. T. Walsh, M. C. Walsh, K. M. Speirs, E. Chiffoleau, C. G. King, W. W. Hancock, J. H. Caamano, C. A. Hunter, P. Scott, L. A. Turka, and Y. Choi. 2003. TRAF6 is a critical factor for dendritic cell maturation and development. *Immunity* 19:353-363.
16. Deng, L., C. Wang, E. Spencer, L. Yang, A. Braun, J. You, C. Slaughter, C. Pickart, and Z. J. Chen. 2000. Activation of the IkappaB kinase complex by TRAF6 requires a dimeric ubiquitin-conjugating enzyme complex and a unique polyubiquitin chain. *Cell* 103:351-361.
17. Wang, C., L. Deng, M. Hong, G. R. Akkaraju, J. Inoue, and Z. J. Chen. 2001. TAK1 is a ubiquitin-dependent kinase of MKK and IKK. *Nature* 412:346-351.
18. Kanayama, A., R. B. Seth, L. Sun, C. K. Ea, M. Hong, A. Shaito, Y. H. Chiu, L. Deng, and Z. J. Chen. 2004. TAB2 and TAB3 activate the NF-kappaB pathway through binding to polyubiquitin chains. *Mol Cell* 15:535-548.
19. Kawai, T., and S. Akira. 2007. TLR signaling. *Semin Immunol* 19:24-32.
20. Pearce, E. L., M. C. Walsh, P. J. Cejas, G. M. Harms, H. Shen, L. S. Wang, R. G. Jones, and Y. Choi. 2009. Enhancing CD8 T-cell memory by modulating fatty acid metabolism. *Nature* 460:103-107.
21. Davis, J. M., H. Clay, J. L. Lewis, N. Ghori, P. Herbomel, and L. Ramakrishnan. 2002. Real-time visualization of mycobacterium-macrophage interactions leading to initiation of granuloma formation in zebrafish embryos. *Immunity* 17:693-702.
22. van der Sar, A. M., R. J. Musters, F. J. van Eeden, B. J. Appelmelk, C. M. Vandenbroucke-Grauls, and W. Bitter. 2003. Zebrafish embryos as a model host for the real time analysis of Salmonella typhimurium infections. *Cell Microbiol* 5:601-611.
23. Ward, A. C., D. O. McPhee, M. M. Condron, S. Varma, S. H. Cody, S. M. Onnebo, B. H. Paw, L. I. Zon, and G. J. Lieschke. 2003. The zebrafish spi1 promoter drives myeloid-specific expression in stable transgenic fish. *Blood* 102:3238-3240.

24. Mathias, J. R., B. J. Perrin, T. X. Liu, J. Kanki, A. T. Look, and A. Huttenlocher. 2006. Resolution of inflammation by retrograde chemotaxis of neutrophils in transgenic zebrafish. *J Leukoc Biol* 80:1281-1288.
25. Redd, M. J., G. Kelly, G. Dunn, M. Way, and P. Martin. 2006. Imaging macrophage chemotaxis in vivo: studies of microtubule function in zebrafish wound inflammation. *Cell Motil Cytoskeleton* 63:415-422.
26. Renshaw, S. A., C. A. Loynes, D. M. Trushell, S. Elworthy, P. W. Ingham, and M. K. Whyte. 2006. A transgenic zebrafish model of neutrophilic inflammation. *Blood* 108:3976-3978.
27. Meijer, A. H., A. M. van der Sar, C. Cunha, G. E. Lamers, M. A. Laplante, H. Kikuta, W. Bitter, T. S. Becker, and H. P. Spaink. 2008. Identification and real-time imaging of a myc-expressing neutrophil population involved in inflammation and mycobacterial granuloma formation in zebrafish. *Dev Comp Immunol* 32:36-49.
28. Hall, C., M. V. Flores, K. Crosier, and P. Crosier. 2009. Live cell imaging of zebrafish leukocytes. *Methods Mol Biol* 546:255-271.
29. Meijer, A. H., S. F. Gabby Krens, I. A. Medina Rodriguez, S. He, W. Bitter, B. Ewa Snaar-Jagalska, and H. P. Spaink. 2004. Expression analysis of the Toll-like receptor and TIR domain adaptor families of zebrafish. *Mol Immunol* 40:773-783.
30. Murayama, E., K. Kissa, A. Zapata, E. Mordelet, V. Briolat, H. F. Lin, R. I. Handin, and P. Herbomel. 2006. Tracing hematopoietic precursor migration to successive hematopoietic organs during zebrafish development. *Immunity* 25:963-975.
31. Stein, C., M. Caccamo, G. Laird, and M. Leptin. 2007. Conservation and divergence of gene families encoding components of innate immune response systems in zebrafish. *Genome Biol* 8:R251.
32. Meeker, N. D., and N. S. Trede. 2008. Immunology and zebrafish: spawning new models of human disease. *Dev Comp Immunol* 32:745-757.
33. Stockhammer, O. W., A. Zakrzewska, Z. Hegedus, H. P. Spaink, and A. H. Meijer. 2009. Transcriptome profiling and functional analyses of the zebrafish embryonic innate immune response to Salmonella infection. *J Immunol* 182:5641-5653.
34. Herbomel, P., B. Thisse, and C. Thisse. 1999. Ontogeny and behaviour of early macrophages in the zebrafish embryo. *Development* 126:3735-3745.
35. Herbomel, P., B. Thisse, and C. Thisse. 2001. Zebrafish early macrophages colonize cephalic mesenchyme and developing brain, retina, and epidermis through a M-CSF receptor-dependent invasive process. *Dev Biol* 238:274-288.
36. Willett, C. E., A. Cortes, A. Zuasti, and A. G. Zapata. 1999. Early hematopoiesis and developing lymphoid organs in the zebrafish. *Dev Dyn* 214:323-336.
37. Davidson, A. J., and L. I. Zon. 2004. The 'definitive' (and 'primitive') guide to zebrafish hematopoiesis. *Oncogene* 23:7233-7246.
38. Lam, S. H., H. L. Chua, Z. Gong, T. J. Lam, and Y. M. Sin. 2004. Development and maturation of the immune system in zebrafish, Danio rerio: a gene expression profiling, in situ hybridization and immunological study. *Dev Comp Immunol* 28:9-28.
39. Phelps, H. A., and M. N. Neely. 2005. Evolution of the zebrafish model: from development to immunity and infectious disease. *Zebrafish* 2:87-103.
40. Lesley, R., and L. Ramakrishnan. 2008. Insights into early mycobacterial pathogenesis from the zebrafish. *Curr Opin Microbiol* 11:277-283.
41. Hegedus, Z., A. Zakrzewska, V. C. Agoston, A. Ordas, P. Racz, M. Mink, H. P. Spaink, and A. H. Meijer. 2009. Deep sequencing of the zebrafish transcriptome response to mycobacterium infection. *Mol Immunol* 46:2918-2930.
42. Wu, H., K. Kerr, X. Cui, and G. A. Churchill. 2003. MAANOVA: A Sofware Package for the Analysis of Spotted cDNA Microarray Experiments.
43. Kerr, M. K., M. Martin, and G. A. Churchill. 2000. Analysis of variance for gene expression microarray data. *J Comput Biol* 7:819-837.
44. Benjamini, Y., and Y. Hochberg. 1995. Controlling the False Discovery Rate: a Practical and Powerful Approach to Multiple Testing. *J.R. Statist. Coc. B.* 57:289-300.
45. Beisvag, V., F. K. Junge, H. Bergum, L. Jolsum, S. Lydersen, C. C. Gunther, H. Ramampiaro, M. Langaas, A. K. Sandvik, and A. Laegreid. 2006. GeneTools--application for functional annotation and statistical hypothesis testing. *BMC Bioinformatics* 7:470.
46. Dahlquist, K. D., N. Salomonis, K. Vranizan, S. C. Lawlor, and B. R. Conklin. 2002. GenMAPP, a new tool for viewing and analyzing microarray data on biological pathways. *Nat Genet* 31:19-20.
47. Xiao, C., J. H. Shim, M. Kluppel, S. S. Zhang, C. Dong, R. A. Flavell, X. Y. Fu, J. L. Wrana, B. L. Hogan, and S. Ghosh. 2003. Ecsit is required for Bmp signaling and mesoderm formation during mouse embryogenesis. *Genes Dev* 17:2933-2949.
48. Mortazavi, A., B. A. Williams, K. McCue, L. Schaeffer, and B. Wold. 2008. Mapping and quantifying mammalian transcriptomes by RNA-Seq. *Nat Methods* 5:621-628.
49. Asmann, Y. W., M. B. Wallace, and E. A. Thompson. 2008. Transcriptome profiling using next-generation sequencing. *Gastroenterology* 135:1466-1468.
50. Sundaram, K., R. Nishimura, J. Senn, R. F. Youssef, S. D. London, and S. V. Reddy. 2007. RANK ligand signal-

ing modulates the matrix metalloproteinase-9 gene expression during osteoclast differentiation. *Exp Cell Res* 313:168-178.

51. Witten, P. E., A. Hansen, and B. K. Hall. 2001. Features of mono- and multinucleated bone resorbing cells of the zebrafish Danio rerio and their contribution to skeletal development, remodeling, and growth. *J Morphol* 250:197-207.
52. Koening, C. L., J. C. Miller, J. M. Nelson, D. M. Ward, J. P. Kushner, L. K. Bockenstedt, J. J. Weis, J. Kaplan, and I. De Domenico. 2009. Toll-like receptors mediate induction of hepcidin in mice infected with Borrelia burgdorferi. *Blood* 114:1913-1918.
53. Ahmad, R., J. Sylvester, and M. Zafarullah. 2007. MyD88, IRAK1 and TRAF6 knockdown in human chondrocytes inhibits interleukin-1-induced matrix metalloproteinase-13 gene expression and promoter activity by impairing MAP kinase activation. *Cell Signal* 19:2549-2557.
54. Volkman, H. E., T. C. Pozos, J. Zheng, J. M. Davis, J. F. Rawls, and L. Ramakrishnan. Tuberculous granuloma induction via interaction of a bacterial secreted protein with host epithelium. *Science* 327:466-469.
55. Solis, M., P. Wilkinson, R. Romieu, E. Hernandez, M. A. Wainberg, and J. Hiscott. 2006. Gene expression profiling of the host response to HIV-1 B, C, or A/E infection in monocyte-derived dendritic cells. *Virology* 352:86-99.
56. O'Prey, J., J. Skommer, S. Wilkinson, and K. M. Ryan. 2009. Analysis of DRAM-related proteins reveals evolutionarily conserved and divergent roles in the control of autophagy. *Cell Cycle* 8:2260-2265.
57. Crighton, D., S. Wilkinson, J. O'Prey, N. Syed, P. Smith, P. R. Harrison, M. Gasco, O. Garrone, T. Crook, and K. M. Ryan. 2006. DRAM, a p53-induced modulator of autophagy, is critical for apoptosis. *Cell* 126:121-134.
58. Munz, C. 2009. Enhancing immunity through autophagy. *Annu Rev Immunol* 27:423-449.
59. Kumar, D., L. Nath, M. A. Kamal, A. Varshney, A. Jain, S. Singh, and K. V. Rao. genome-wide analysis of the host intracellular network that regulates survival of Mycobacterium tuberculosis. *Cell* 140:731-743.
60. Wu, S., L. Page, and N. M. Sherwood. 2006. A role for GnRH in early brain regionalization and eye development in zebrafish. *Mol Cell Endocrinol* 257-258:47-64.
61. Chen, H. F., E. B. Jeung, M. Stephenson, and P. C. Leung. 1999. Human peripheral blood mononuclear cells express gonadotropin-releasing hormone (GnRH), GnRH receptor, and interleukin-2 receptor gamma-chain messenger ribonucleic acids that are regulated by GnRH in vitro. *J Clin Endocrinol Metab* 84:743-750.
62. Tanriverdi, F., L. F. Silveira, G. S. MacColl, and P. M. Bouloux. 2003. The hypothalamic-pituitary-gonadal axis: immune function and autoimmunity. *J Endocrinol* 176:293-304.
63. Min, J. Y., M. H. Park, J. K. Lee, H. J. Kim, and Y. K. Park. 2009. Gonadotropin-releasing hormone modulates immune system function via the nuclear factor-kappaB pathway in murine Raw264.7 macrophages. *Neuroimmunomodulation* 16:177-184.
64. Chakraborty, A., H. Brooks, P. Zhang, W. Smith, M. R. McReynolds, J. B. Hoying, R. Bick, L. Truong, B. Poindexter, H. Lan, W. Elbjeirami, and D. Sheikh-Hamad. 2007. Stanniocalcin-1 regulates endothelial gene expression and modulates transendothelial migration of leukocytes. *Am J Physiol Renal Physiol* 292:F895-904.
65. Yoshiko, Y., N. Maeda, and J. E. Aubin. 2003. Stanniocalcin 1 stimulates osteoblast differentiation in rat calvaria cell cultures. *Endocrinology* 144:4134-4143.
66. Wellen, K. E., R. Fucho, M. F. Gregor, M. Furuhashi, C. Morgan, T. Lindstad, E. Vaillancourt, C. Z. Gorgun, F. Saatcioglu, and G. S. Hotamisligil. 2007. Coordinated regulation of nutrient and inflammatory responses by STAMP2 is essential for metabolic homeostasis. *Cell* 129:537-548.